Vol 15 No 4, April 2006
1009-1963/2006/15(04)/0872-06

Chinese Physics

© 2006 Chin. Phys. Soc.
and IOP Publishing Ltd

Metastable phase separation and rapid solidification of undercooled Co-Cu alloy under different conditions

Cao Chong-De(曹崇德)†

Department of Applied Physics, Northwestern Polytechnical University, Xi'an 710072, China

(Received 8 November 2005; revised manuscript received 19 December 2005)

The metastable liquid phase separation and rapid solidification behaviours of $Co_{61.8}Cu_{38.2}$ alloy were investigated by using differential thermal analysis (DTA) in combination with glass fluxing, electromagnetic levitation (EML) and drop tube techniques. It is found that the liquid phase separation process and the solidification microstructures intensively depend on the experimental processing parameters, such as undercooling level, cooling rate, gravity level, liquid surface tension and the wetting state of crucible. Large undercooling and surface tension difference of the two liquids tend to facilitate further separation and cause severe macrosegregation. On the other hand, rapid cooling and low gravity effectively suppress the coalescence of the minority phase. Severe macrosegregation patterns are formed in the bulk samples processed by both DTA and EML. In contrast, disperse structures with fine spherical Cu-rich spheres homogeneously distributed in the matrix of Co-rich phase have been obtained in drop tube.

Keywords: crystal growth, metastable phase separation, undercooling, rapid solidification
PACC: 8130F, 8130D, 6470J

1. Introduction

The Co–Cu alloy system is well known as a peritectic system, but shows a metastable miscibility gap in the undercooled state.[1,2] Once a uniform Co-Cu alloy melt is undercooled into the miscibility gap, it separates into two liquids: one Co-rich and the other Cu-rich. Intensive understanding of the dynamics of the metastable phase separation has proven to be of great importance for microstructure control and thus gives the opportunity of industrial exploitation, such as potential application prospects as a high temperature bearing material and a new high performance magnetic material. Much work has been devoted to microstructure evolution and quantitative determination of the metastable miscibility gap boundary on the basis of magnetic susceptibility measurement,[1] electromagnetic levitation (EML),[3−6] differential thermal analysis (DTA)[4] and glass-fluxing processing.[7] However, little quantitative information is available on systematic analysis of the effect of processing parameters on the metastable phase separation and structure evolution.[8,9] A quantitative analysis is needed for the demixing and subsequent solidification.

In the present work, DTA combining with glass fluxing was used to directly determine the critical metastable phase separation temperature. The containerless processing through EML allows for achievement of high bulk undercooling and in situs observation of solidification process. The drop tube technique provides a unique way for investigating metastable phase transformation, especially for liquid phase separation and coalescence characteristics, by combining rapid cooling with low gravity effect.[10,11] Microstructure evolution and the effect of processing parameters on phase separation and solidification are discussed in this work.

2. Experimental procedures

The alloy samples were prepared by alloying highly pure Co (99.998%) and Cu (99.999%) in an arc-melting furnace. Each sample for EML and drop tube is 1–1.2g in mass, and that for DTA 250–350mg. DTA

†E-mail: caocd@nwpu.edu.cn

measurements were performed by a Netzsch DTA 404S differential thermal analyser at heating and cooling rates of +0.17K/s and −0.33K/s, with Duran glass as fluxing agent. The heating and cooling process was repeated for 5 times during the DTA measurements. The detailed descriptions of DTA experimental procedures were presented elsewhere.[4] In the EML processing, the specimen was heated above the liquidus temperature and cooled by a He–H_2 gas flow. Solidification of the levitated sample spontaneously initiated without triggering. A He-filled drop tube, 8 m in length, was employed to examine solidification of small droplets. The bulk specimen was contained in a quartz tube with a small orifice at its lower end and fixed on the top of the drop tube. The sample was melted and overheated by induction, and then, was ejected through the orifice and dispersed into many fine droplets by exerting a high pressure gas flow of Argon into the quartz tube. The bulk samples and the small droplets were examined with respect to structures and concentration profiles by means of an SEM Stereoscan 360 from Leica/Cambridge Instruments.

3. Results and discussions

Figure 1 shows the phase diagram of the Co-Cu alloy system, superposed region is the metastable miscibility gap boundary determined by DTA[4] and undercoolings of $Cu_{61.8}Co_{38.2}$ alloy obtained by DTA, EML and drop tube. The liquidus temperature of

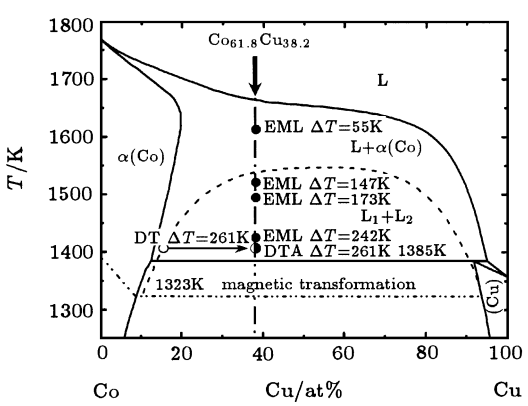


Fig.1. Undercoolings of $Cu_{61.8}Co_{38.2}$ alloy shown in the Co-Cu phase diagram.

$Cu_{61.8}Co_{38.2}$ alloy is 1667 K. When solidification occurs above the miscibility gap boundary, primary α(Co) phase is formed and the composition of the liquid phase changes according to the equilibrium liquidus curve. A peritectic transformation subsequently takes place between primary α(Co) phase and the remnant liquid phase at 1385 K. Once the alloy melt is undercooled into the miscibility gap, the homogeneous melt separates into two liquids, L_1(Co-rich) and L_2(Cu-rich).

The thermal information on metastable liquid phase separation of undercooled $Cu_{61.8}Co_{38.2}$ alloy is revealed by the DTA cooling trace, where the demixing is manifested as a small step in the exothermic direction, as presented in Fig.2(a). We designate the characteristic onset temperature of this process as T_{sep}, which is identified as 1538 K for $Cu_{61.8}Co_{38.2}$ alloy. After the onset of liquid phase separation, the DTA signal retains its exothermic offset during further cooling. This shows that the concentration change in both separated phases continues until the rapid solidification of the Co-rich liquid occurs. This sample was undercooled by 261 K below its equilibrium liquidus temperature and solidified at 1406 K. Subsequently, peritectic transformation occurred near the equilibrium peritectic temperature. Figure 2(b) presents the corresponding structural morphology. Obviously, a severe macrosegregation pattern has been formed. The Co-rich phase was completely coagulated into a large sphere, occupying the most volume of the sample. Except for one large and many small Cu-rich spherulites embedded in the L_1 phase, most of the L_2 phase is distributed at the outer surface of the sample. The density of liquid Co is slightly higher than that of liquid Cu at a high temperature.[12] Therefore, there is a tendency that the Cu-rich liquid L_2 goes up, causing the fact that the big L_2 droplet was located near the sample top. The Cu-rich liquid phase has stronger abilities of wetting the glass and smaller surface tension than the Co-rich liquid, resulting in the migration of the Cu-rich liquid towards the sample surface. However, this sample is not completely encased by the molten glass. Consequently, surface segregation of the Cu-rich phase occurs at the lower part of the sample.

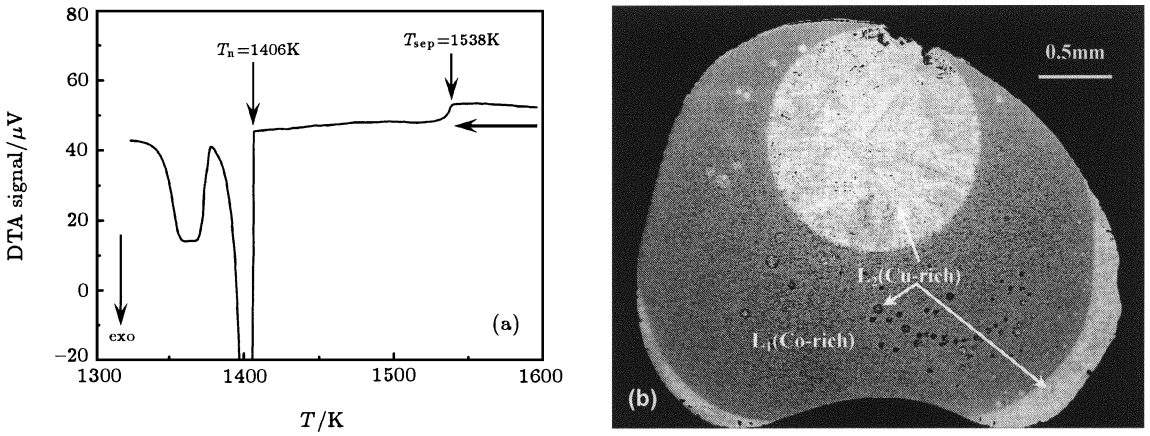


Fig.2. DTA cooling curve and the corresponding solidified structure: (a) DTA cooling curve; (b) structural morphology of the bulk sample undercooled by 261K in the DTA measurement (etched by a solution of 5g $FeCl_3$+ 10ml HCl + 100ml alcohol).

By using EML technique, undercoolings of 7–242 K were obtained for $Cu_{61.8}Co_{38.2}$ alloy melt. Figure 3 presents the temperature–time profiles measured by a pyrometer on two bulk samples containerlessly processed by EML and undercooled by 55 K and 242 K respectively. In the case of ΔT=55 K, the alloy melt solidified without demixing at 1612 K and the sample temperature rose nearly to the equilibrium liquidus temperature due to recalescence. In the case of a large undercooling of 242 K, the cooling rate was decreased appreciably by the exothermic liquid phase separation, which took place at T_{sep}=1538 K and lasted until solid nucleation was initiated at T_n=1425 K. The separated liquid droplets grow and coagulate between T_{sep} and T_n, and the concentrations of both separated liquids change following the metastable miscibility gap boundary. At the nucleation temperature 1425 K, the Co-rich liquid contains 16.92at% Cu and has an undercooling of 287 K according to the metastable miscibility gap boundary and the equilibrium liquidus line respectively. Once the Co-rich liquid phase nucleates, sharp recalescence takes place and brings on a temperature rise of 185 K. The relationship between recalescence induced temperature rise ΔT_R and undercooling level ΔT is shown in Fig.4. As undercooling increases, the temperature rise linearly increases because of the enhancement of recalescence. It is apparent that the slope of the ΔT_R-ΔT function in the case of demixing is smaller than that in the case of solidification occurring above the critical demixing temperature. This phenomenon may be due to the surface segregation of Cu-rich phase at high undercoolings.

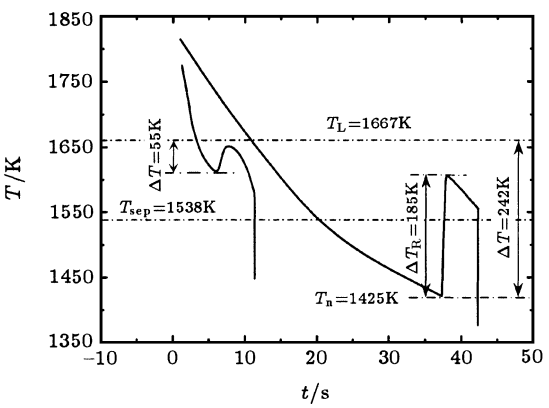


Fig.3. Temperature-time profiles measured during EML processing.

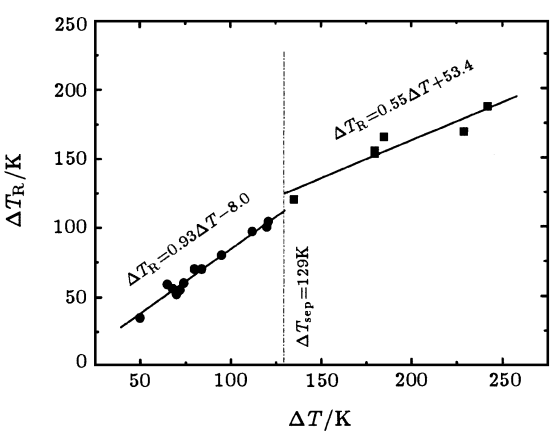


Fig.4. Temperature rise resulting from recalescence as functions of undercooling during EML processing.

The structural morphologies of $Co_{61.8}Cu_{38.2}$ alloy samples processed by EML are strongly dependent on undercooling level. When the alloy melt solidifies above the critical liquid phase separation temperature, i.e. $\Delta T < \Delta T_{sep}$=129 K, normal peritectic structures are obtained, as demonstrated in Fig.5(a). Herein, the undercooling is only 55 K, and the microstructure is characterized by coarse primary α-Co dendrites with interdendritic (Cu) phase. The maximum grain size $d_{\alpha-Co}$ of primary α-Co phase attains 193 μm in this sample. With the increase of undercooling, primary α-Co phase is significantly refined as a result of enhanced dendrite fragmentation during recalescence, as shown in the inserted figure in Fig.5(a).

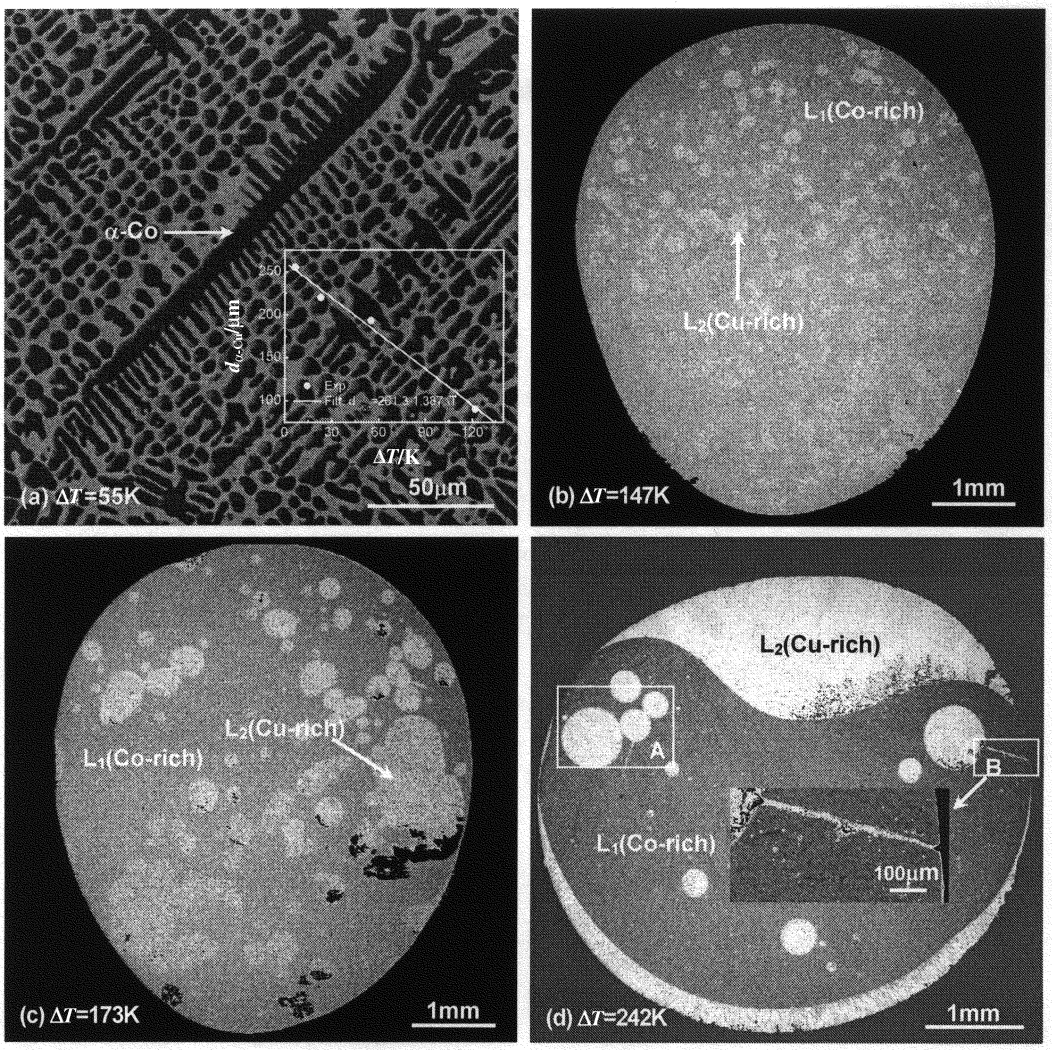


Fig.5. Structures of $Co_{61.8}Cu_{38.2}$ alloy processed by EML at various undercoolings.

When $Co_{61.8}Cu_{38.2}$ alloy melt is undercooled into the range of the metastable miscibility gap, it separates into L_1 phase and L_2 phase. The high undercooling level causes rapid solidification, which freezes the metastable states. Structures formed after liquid phase separation and solidified at various undercoolings are shown in Figs.5(b), (c) and (d). At a relatively small undercooling of 147 K, which is just slightly larger than the critical undercooling for metastable demixing, the minority phase L_2 spherulites, with diameters smaller than 300 μm, are homogeneously distributed in the matrix of the majority phase L_1. At a larger undercooling of 173 K, the number of L_2 spherulites is much smaller than that in the case of ΔT=147 K, and the maximum L_2 sphere attains 1600μm in diameter. It can be seen that some L_2 spheres are located at the sample surface. This surface segregation of Cu-rich liquid was well developed at a large undercooling of 242 K, as presented in Fig.5(d). The L_2 phase was strongly coagulated by multiple col-

lision and most of this phase segregated to the surface to form a Cu-rich layer. It is noted that most Cu-rich phase is located at the upper part of the sample, which shows that the effect of the gravity on phase separation is still obvious in the EML containerless processing. The coagulation of the minority phase by collision was frozen in, as revealed by the region marked as A. It is known that Co-Cu alloy melts exhibit a strong concentration dependence of surface tension. With the increase of Cu content, the surface tension of liquid Co-Cu alloys decreases drastically.[13] The Cu-rich liquid L_2 has a much lower surface tension than the Co-rich liquid L_1, and thus, the L_2 liquid tends to migrate outwards and wet the sample surface. Such a surface segregation process is evidenced by a channel between a L_2 droplet and the L_2 layer at the outer surface, as shown in the inserted figure in Fig.5(d).

The inverted secondary electron micrograph in Fig.6 shows typical microstructure formed in the droplets solidified in the drop tube, which is significantly different from those of bulk samples processed by DTA and EML. The L_2 spherulites are much finer and more disperse and their maximum diameter is only 7 μm. As a result of reduced gravity effect, gravity-induced sedimentation has been suppressed. However, some other factors dominate the liquid phase separation process. At the droplet surface there is a thin layer of Cu-rich phase with a thickness of 2–3μm and with the same concentration as the inner L_2 spheres, which indicates that the surface segregation of Cu-rich phase still takes place under such rapid cooling conditions. In the helium-filled drop tube, the cooling rate at the droplet surface should be higher than that of the inner part,[14] and thus the solidification is initiated from the droplet surface. The Cu-rich spheres near the droplet surface were segregated to the surface or pushed inward by the rapidly growing Co-rich crystals, which led to a Co-rich shell of about 14 μm in thickness near the droplet surface. Energy dispersive spectrometry measurements indicate that the L_1(Co-rich) matrix contains 15.5 at% Cu. Thus, from the metastable phase diagram we can indirectly make out that this droplet solidified at an undercooling of 261 K. Although this droplet solidified at the same undercooling as the DTA processed sample shown in Fig.2 (b), their structures are distinct. The main factors leading to such difference in structure formation in these two cases are cooling rate, gravity level and wetting conditions.

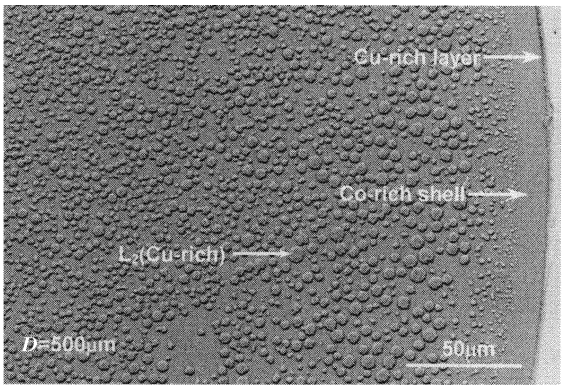


Fig.6. Inverted secondary electron image showing microstructures of a droplet solidified in the drop tube (etched by a solution of 5g $FeCl_3$+ 10ml HCl + 100ml alcohol).

Figure 7 gives the maximum diameter d_{L2} of Cu-rich spheres formed in the drop tube as a function of droplet size. It is evident that Cu-rich spheres are remarkably refined when droplet size decreases. This demonstrates that rapid cooling suppresses the coagulation of the minority phase and facilitates the achievement of disperse structures.

When liquid phase separation occurs, the separated liquids with different compositions are all in the undercooled state corresponding to their liquidus temperatures. Therefore, in all the cases that this alloy is processed by DTA, EML and drop tube, once the Co-rich liquid solidifies, α(Co) phase will precipitate from the L_2 (Cu-rich) liquid and peritectic transformation will occur subsequently.

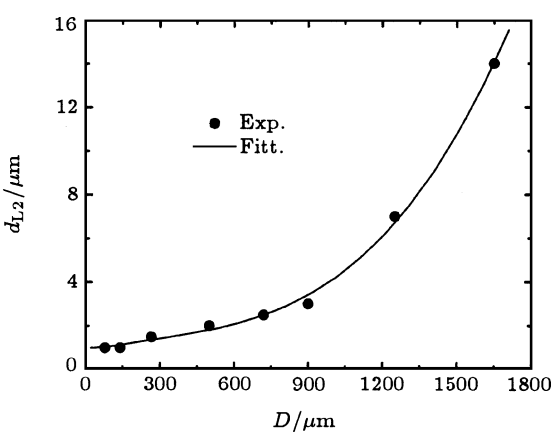


Fig.7. Maximum diameter of Cu-rich spheres formed in the drop tube.

4. Conclusions

The metastable phase separation and rapid solidification of undercooled $Cu_{61.8}Co_{38.2}$ alloy have been accomplished by DTA, EML and drop tube processing. The critical liquid phase separation temperature

is accurately determined to be 1538 K by DTA in combination with glass fluxing. It is found that undercooling level, cooling rate, gravity level and surface tension difference between the two separated phases play a dominant role in the coalescence and segregation of the minority phase. Enhanced undercooling has the effect of facilitating the metastable phase separation, whereas rapid cooling and low gravity tend to restrain the multiple collision and coagulation of the minority phase droplets, which results in fine and disperse structures in the droplets solidified during free fall in drop tube. However, the difference in surface tension of the two separated liquids leads to surface segregation of Cu-rich phase in drop tube processing. Macrosegregation morphologies induced by surface tension difference and gravity are observed in both DTA and EML processed samples.

Acknowledgement

The author is grateful to Professor D. M. Herlach, Dr G. P. Görler and Professor B. Wei for their support and helpful discussions.

References

[1] Xu J F and Wei B 2005 *Acta Phys. Sin.* **54** 3444
[2] Nishizawa T and Ishida K 1984 *Bull. Alloy Phase Diagrams* **5** 161
[3] Munitz A and Abbaschian R 1996 *Metall. Mater. Trans.* A **27** 4049
[4] Cao C D, Görler G P, Herlach D M and Wei B 2002 *Mater. Sci. Eng.* A **325** 503
[5] Kim D I and Abbaschian R 2000 *J. Phase Equilibria* **21** 25
[6] Dong C, Wei B, Leonhardt M, Lindendreuz H G and Löser W 1998 *Inter. J. Non-Equilibrium Processing* **10** 241
[7] Cao C D and Görler G P 2005 *Chin. Phys. Lett.* **22** 482
[8] Cao C D, Wang N and Wei B 2000 *Sci. Chin.* A **43** 1318
[9] Wang C P, Liu X J, Ohnuma I, Kainuma R and Ishida K 2002 *Science* **297** 990
[10] Jakse N, Le Bacq O and Pasturel A 2004 *Phys. Rev.* B **70** 174203
[11] Liu X R, Cao C D and Wei B 2003 *Chin. Phys.* **12** 1266
[12] Iida T and Guthrie R I L 1993 *The Physical Properties of Liquid Metals* (Oxford: Clarendon)
[13] Eichel R A and Egry I 1999 *Z. Metallkde.* **90** 371
[14] Fransaer J, Wagner A V and Spaepen F 2000 *J. Appl. Phys.* **87** 1801